

Copyright © 1995, by the author(s).
All rights reserved.

Permission to make digital or hard copies of all or part of this work for personal or classroom use is granted without fee provided that copies are not made or distributed for profit or commercial advantage and that copies bear this notice and the full citation on the first page. To copy otherwise, to republish, to post on servers or to redistribute to lists, requires prior specific permission.

**2D ELECTROMAGNETICS AND PIC
ON A QUADRILATERAL MESH**

by

A. Bruce Langdon

Memorandum No. UCB/ERL M95/96

5 December 1995

AFOSR Grant F49620-92-J-0487 (OOPIC)

**2D ELECTROMAGNETICS AND PIC
ON A QUADRILATERAL MESH**

by

A. Bruce Langdon

Memorandum No. UCB/ERL M95/96

5 December 1995

ELECTRONICS RESEARCH LABORATORY

College of Engineering
University of California, Berkeley
94720

2D electromagnetics and PIC on a quadrilateral mesh

A. Bruce Langdon¹

Electronics Research Laboratory, University of California, Berkeley, CA 94720, USA

Abstract

At least three schemes for evolving the electromagnetic fields on a nonorthogonal mesh have turned out to be weakly unstable, as seen in long runs. In contrast, sufficient conditions for stability will be shown for my formulation of Maxwell's equations on a nonorthogonal quadrilateral mesh. Here, stability means for example that cavity oscillations have exactly zero growth (or decay) for any time step up to a Courant limit whose value is easily calculated. For larger time steps, there is an odd-even instability.

In this formulation, we consider separately the cell fluxes of D, B and line integrals of E, H . For the closure of Maxwell's equations we need linear transformations of D to E and B to H . Stability and certain conservation laws are dependent on these linear transformations being symmetric and non-negative. These properties can be regarded as constraints while one is choosing the linear transformations to achieve accuracy. Boundary conditions can undermine such nice features.

There is some discussion of coupling of particles and fields.

Introduction

In my Annapolis talk [1], I showed how one can learn what is needed to build conservation laws into the discrete representation of Maxwell's equations. Then the mesh was near-orthogonal. Now I want to separate out the generic aspects from those which, for example, provide accuracy in a non-orthogonal quadrilateral mesh.

Here the 2D mesh is quadrilateral and field locations are staggered, in generalization of the rectangular Yee mesh. I separate aspects of the discretization that provide the equations of evolution and conservation laws from the details of a particular difference or finite-element representation.² Later I outline a straw-man.

A partial implementation is described in [3].

Field Variables and Maxwell's equations

In earlier work[1], on how to ensure the existence of conservation laws, etc., I found that certain products of fields with lengths (line integrals) or areas (fluxes) arise repeatedly in the equations of evolution and in the sums that define e.g. the field energy. Eastwood et al [4] use *separate variables* for these same fluxes and line integrals, and generalize the constitutive relations to include mesh metric information. I use a different notation, and introduce cell capacitances and inductances instead of speaking of constitutive relations, but the benefits are the same in brevity and help clarify the issues of conservation laws and accuracy.

The Ampere-Maxwell and Faraday equations relate rate of change of *fluxes* of B and D to *line integrals* of E and H .

$$\oint \mathbf{dr} \cdot \mathbf{H} = I + \frac{d}{dt} \int_S \mathbf{dS} \cdot \mathbf{D} \quad (1a)$$

$$\oint \mathbf{dr} \cdot \mathbf{E} = -\frac{d}{dt} \int_S \mathbf{dS} \cdot \mathbf{B} \quad (1b)$$

$$\int_S \mathbf{dS} \cdot \mathbf{D} = Q, \quad \int_S \mathbf{dS} \cdot \mathbf{B} = 0 \quad (1cd)$$

¹ Also at X division, Physics Department, Lawrence Livermore National Laboratory, Livermore, CA 94550, USA.

² This work was inspired in part by my "circuit mesh interpretation of 2D orthogonal mesh EM", [1], and by Eastwood's talk at GMU [2].

where current $I = \int_S d\mathbf{S} \cdot \mathbf{J}$ and enclosed charge $Q = \int_V dr \rho$ satisfy a continuity equation $dQ/dt + I = 0$ when S is a closed surface enclosing V .

We consider 2D fields, in cartesian x, y , or cylindrical z, r coordinates. For now consider only E_x, E_y, B_z or E_z, E_r, B_φ , respectively. These are called the TM fields by some. Define line and surface integrals as follows (noting also the simplest representation of each in z, r):

$$\mathcal{E}_1 = \text{line integral of } E \text{ along side of cell; } \mathcal{E}_1 = E_1(h_1\Delta x_1)$$

$$\mathcal{H}_\varphi = \text{line integral of } H \text{ around hoop; } \mathcal{H}_\varphi = 2\pi r B_\varphi / \mu_0$$

$$\mathcal{D}_1 = \text{flux of } D = \epsilon_0 E \text{ through sides of cell; } \mathcal{D}_1 = \epsilon_0(2\pi r h_2 \Delta x_2) E_1$$

$$I_1 = \text{flux of } J \text{ through sides of cell; } I_1 = (2\pi r h_2 \Delta x_2) J_1$$

$$\mathcal{B}_\varphi = \text{flux of } B = \mu_0 H \text{ through cell; } \mathcal{B}_\varphi = (h_1 \Delta x_1 h_2 \Delta x_2) B_\varphi$$

In x, y , the factor $2\pi r$ is absent, and one could understand that the integrals are over unit z .

If the electric field is irrotational,

$$-\mathcal{E}_{1,j+\frac{1}{2},k} = \varphi_{j+1,k} - \varphi_{j,k}, \quad -\mathcal{E}_{2,j,k+\frac{1}{2}} = \varphi_{j,k+1} - \varphi_{j,k} \quad (2)$$

so \mathcal{E} is a potential difference in that case.

These relations that follow from the field equations are exact, though not applicable by themselves:

$$\left[\frac{d\mathcal{B}_\varphi}{dt} \right]_{j+\frac{1}{2},k+\frac{1}{2}} = (\mathcal{E}_1)_{j+\frac{1}{2},k+1} - (\mathcal{E}_1)_{j+\frac{1}{2},k} \quad j = 0, N_1 - 1, \quad k = 0, N_2 - 1 \quad (3)$$

$$- (\mathcal{E}_2)_{j+1,k+\frac{1}{2}} + (\mathcal{E}_2)_{j,k+\frac{1}{2}}$$

$$\left[\frac{d\mathcal{D}_1}{dt} \right]_{j+\frac{1}{2},k} = (\mathcal{H}_\varphi)_{j+\frac{1}{2},k+\frac{1}{2}} - (\mathcal{H}_\varphi)_{j+\frac{1}{2},k-\frac{1}{2}} - I_{1,j+\frac{1}{2},k}, \quad j = 0, N_1 - 1, \quad k = 1, N_2 - 1 \quad (4a)$$

$$\left[\frac{d\mathcal{D}_2}{dt} \right]_{j,k+\frac{1}{2}} = -(\mathcal{H}_\varphi)_{j+\frac{1}{2},k+\frac{1}{2}} + (\mathcal{H}_\varphi)_{j-\frac{1}{2},k+\frac{1}{2}} - I_{2,j,k+\frac{1}{2}}, \quad j = 1, N_1 - 1, \quad k = 0, N_2 - 1 \quad (4b)$$

$$Q_{j,k} = (\mathcal{D}_1)_{j+\frac{1}{2},k} - (\mathcal{D}_1)_{j-\frac{1}{2},k} \quad j = 1, N_1 - 1, \quad k = 1, N_2 - 1 \quad (5)$$

$$+ (\mathcal{D}_2)_{j,k+\frac{1}{2}} - (\mathcal{D}_2)_{j,k-\frac{1}{2}}$$

The Maxwell relations for the other half of the fields, called the TE fields by some, are:

$$\left[\frac{d\mathcal{D}_\varphi}{dt} \right]_{j,k} = (\mathcal{H}_2)_{j+\frac{1}{2},k} - (\mathcal{H}_2)_{j-\frac{1}{2},k} \quad j = 1, N_1 - 1, \quad k = 1, N_2 - 1 \quad (6)$$

$$- (\mathcal{H}_1)_{j,k+\frac{1}{2}} + (\mathcal{H}_1)_{j,k-\frac{1}{2}} - I_{\varphi,j,k}$$

$$\left[\frac{d\mathcal{B}_2}{dt} \right]_{j+\frac{1}{2},k} = (\mathcal{E}_\varphi)_{j+1,k} - (\mathcal{E}_\varphi)_{j,k} \quad j = 0, N_1 - 1, \quad k = 0, N_2 \quad (7)$$

$$\left[\frac{d\mathcal{B}_1}{dt} \right]_{j,k+\frac{1}{2}} = -(\mathcal{E}_\varphi)_{j,k+1} + (\mathcal{E}_\varphi)_{j,k} \quad j = 0, N_1, \quad k = 0, N_2 - 1$$

$$0 = (\mathcal{B}_2)_{j+\frac{1}{2},k} - (\mathcal{B}_2)_{j-\frac{1}{2},k} \quad j = 1, N_1 - 1, \quad k = 1, N_2 - 1 \quad (8)$$

$$+ (\mathcal{B}_1)_{j,k+\frac{1}{2}} - (\mathcal{B}_1)_{j,k-\frac{1}{2}}$$

Closure

To use these equations to advance the fields in time using “leap-frog” time integration, we need only add boundary conditions and methods for finding \mathcal{H} from \mathcal{B} and \mathcal{E} from \mathcal{D} . Mathematically, we will see that these methods should be symmetric, nonnegative linear transformations. In the OOPIC code, boundary conditions and these methods should be easily replaced, as I believe this formalism concentrates volatility into them.

Orthogonal mesh

In the simplest case, applicable to a locally orthogonal mesh, the linear transformations are diagonal:

$$\mathcal{H}_{\varphi,j+\frac{1}{2},k+\frac{1}{2}} = L_{j+\frac{1}{2},k+\frac{1}{2}}^{-1} \mathcal{B}_{\varphi,j+\frac{1}{2},k+\frac{1}{2}} \quad (10)$$

$$\mathcal{E}_{1,j+\frac{1}{2},k} = C_{j+\frac{1}{2},k}^{-1} \mathcal{D}_{1,j+\frac{1}{2},k}, \quad \mathcal{E}_{2,j,k+\frac{1}{2}} = C_{j,k+\frac{1}{2}}^{-1} \mathcal{D}_{2,j,k+\frac{1}{2}} \quad (11)$$

I have introduced mesh inductances L and capacitances C , so called because the ratio of a flux \mathcal{D} to potential difference \mathcal{E} is a capacitance, and the ratio of flux \mathcal{B} to current I is an inductance.* C is of the form $\epsilon_0(\text{area})/(\text{length})$ and L is of the form $\mu_0(\text{area})/(\text{length})$. For a cartesian x, y rectangular mesh,

$$C_{j+\frac{1}{2},k} = \epsilon_0 \Delta y / \Delta x, \quad C_{j,k+\frac{1}{2}} = \epsilon_0 \Delta x / \Delta y, \quad L_{j+\frac{1}{2},k+\frac{1}{2}} = \mu_0 \Delta x \Delta y \quad (12)$$

where the ‘unit length in z ’ has not been written in. This is just the Yee type of mesh, in 2-dimensions.

Non-orthogonal mesh

In a non-orthogonal mesh especially, accuracy requires non-diagonal linear transformations.

We can calculate the dispersion relation for a mesh of parallelograms. Without non-diagonal terms, this shows that wave propagation has an error that does not go to zero as the mesh spacing goes to zero, just as in the triangular mesh algorithm analyzed by Rambo [5]. This is demonstrated in a later section of this paper.

What Eastwood et al [4] advocated is equivalent to

$$\begin{aligned} \mathcal{E}_{1,j+\frac{1}{2},k} &= C_{j+\frac{1}{2},k}^{-1} \mathcal{D}_{1,j+\frac{1}{2},k} \\ &+ C_{j+\frac{1}{2},k;j,k-\frac{1}{2}}^{-1} \mathcal{D}_{2,j,k-\frac{1}{2}} + C_{j+\frac{1}{2},k;j+1,k-\frac{1}{2}}^{-1} \mathcal{D}_{2,j+1,k-\frac{1}{2}} \\ &+ C_{j+\frac{1}{2},k;j,k+\frac{1}{2}}^{-1} \mathcal{D}_{2,j,k+\frac{1}{2}} + C_{j+\frac{1}{2},k;j+1,k+\frac{1}{2}}^{-1} \mathcal{D}_{2,j+1,k+\frac{1}{2}} \end{aligned} \quad (15a)$$

$$\begin{aligned} \mathcal{E}_{2,j,k+\frac{1}{2}} &= C_{j,k+\frac{1}{2}}^{-1} \mathcal{D}_{2,j,k+\frac{1}{2}} \\ &+ C_{j,k+\frac{1}{2};j-\frac{1}{2},k}^{-1} \mathcal{D}_{1,j-\frac{1}{2},k} + C_{j,k+\frac{1}{2};j-\frac{1}{2},k+1}^{-1} \mathcal{D}_{1,j-\frac{1}{2},k+1} \\ &+ C_{j,k+\frac{1}{2};j+\frac{1}{2},k}^{-1} \mathcal{D}_{1,j+\frac{1}{2},k} + C_{j,k+\frac{1}{2};j+\frac{1}{2},k+1}^{-1} \mathcal{D}_{1,j+\frac{1}{2},k+1} \end{aligned} \quad (15b)$$

where the coefficients of the off-diagonal terms are, dimensionally, inverse capacitances. The most important aspect of this is that \mathcal{D}_2 contributes to \mathcal{E}_1 and \mathcal{D}_1 to \mathcal{E}_2 in a nonorthogonal mesh. As Eastwood says, it’s like an anisotropic dielectric.

Below we will see nice consequences of keeping the transformation symmetric, $C_{j+\frac{1}{2},k;j,k-\frac{1}{2}} = C_{j,k-\frac{1}{2};j+\frac{1}{2},k}$ and $C_{j+\frac{1}{2},k;j,k+\frac{1}{2}} = C_{j,k+\frac{1}{2};j+\frac{1}{2},k}$, and for Eq. (15) to be a non-negative transformation.

* Eastwood et al [2,4] generalized the constitutive relations to include the geometric factors in ϵ and μ . There’s no difference to code performance.

I have given a little thought toward accuracy improvement possible with simpler non-diagonal couplings. In this simplification, the cross-capacitances are nonzero only if the angle at the nearest cell corner is acute. What is the motivation?

- It may suffice to make dispersion etc. accurate enough
- It may require less storage for capacitances (although one needs a list of non-zero couplings)
- It can make the inverse transformation (\mathcal{D} in terms of \mathcal{E}) very sparse, a help in expressing the Laplacian if Poisson's equation is needed.

Conservation laws

Magnetic flux

From Faraday's law

$$\begin{aligned} \frac{d}{dt} \sum_{j=0}^{N_1-1} \sum_{k=0}^{N_2-1} (\mathcal{B}_\varphi)_{j+\frac{1}{2}, k+\frac{1}{2}} = & - \sum_{j=0}^{N_1-1} [(\mathcal{E}_1)_{j+\frac{1}{2}, 0} - (\mathcal{E}_1)_{j+\frac{1}{2}, N_2}] \\ & + \sum_{k=0}^{N_2-1} [(\mathcal{E}_2)_{0, k+\frac{1}{2}} - (\mathcal{E}_2)_{N_1, k+\frac{1}{2}}] \end{aligned} \quad (20)$$

Poynting theorem (energy conservation)

First, keep time as a continuous variable.

In a continuous, linear medium the energy conservation theorem is

$$\frac{d}{dt} \int_V dr \frac{1}{2} (\mathbf{E} \cdot \mathbf{D} + \mathbf{B} \cdot \mathbf{H}) + \int_V dr \mathbf{J} \cdot \mathbf{E} + \int_S d\mathbf{S} \cdot \mathbf{E} \times \mathbf{H} = 0 \quad (21)$$

Assuming the identities

$$\sum \mathcal{E}_1^{(1)} \mathcal{D}_1^{(2)} + \sum \mathcal{E}_2^{(1)} \mathcal{D}_2^{(2)} = \sum \mathcal{E}_1^{(2)} \mathcal{D}_1^{(1)} + \sum \mathcal{E}_2^{(2)} \mathcal{D}_2^{(1)} \quad \text{and} \quad \sum \mathcal{B}^{(1)} \mathcal{H}^{(2)} = \sum \mathcal{B}^{(2)} \mathcal{H}^{(1)}, \quad (22)$$

which follow from *symmetry* of the linear transformations of \mathcal{D} to \mathcal{E} and \mathcal{B} to \mathcal{H} , we can derive

$$\begin{aligned} & \sum_{j=0}^{N_1-1} \sum_{k=0}^{N_2} \left[\frac{d}{dt} \left(\frac{1}{2} \mathcal{E}_1 \mathcal{D}_1 \right) + \mathcal{E}_1 I_1 \right]_{j+\frac{1}{2}, k} + \sum_{j=0}^{N_1} \sum_{k=0}^{N_2-1} \left[\frac{d}{dt} \left(\frac{1}{2} \mathcal{E}_2 \mathcal{D}_2 \right) + \mathcal{E}_2 I_2 \right]_{j, k+\frac{1}{2}} \\ & + \sum_{j=0}^{N_1-1} \sum_{k=0}^{N_2-1} \left[\frac{d}{dt} \left(\frac{1}{2} \mathcal{B}_\varphi \mathcal{H}_\varphi \right) \right]_{j+\frac{1}{2}, k+\frac{1}{2}} \\ = & + \sum_{j=0}^{N_1-1} (\mathcal{E}_1)_{j+\frac{1}{2}, 0} \left\{ -(\mathcal{H}_\varphi)_{j+\frac{1}{2}, \frac{1}{2}} + \left[I_1 + \frac{d\mathcal{D}_1}{dt} \right]_{j+\frac{1}{2}, 0} \right\} \\ & + \sum_{j=0}^{N_1-1} (\mathcal{E}_1)_{j+\frac{1}{2}, N_2} \left\{ (\mathcal{H}_\varphi)_{j+\frac{1}{2}, N_2-\frac{1}{2}} + \left[I_1 + \frac{d\mathcal{D}_1}{dt} \right]_{j+\frac{1}{2}, N_2} \right\} \\ & + \sum_{k=0}^{N_2-1} (\mathcal{E}_2)_{0, k+\frac{1}{2}} \left\{ (\mathcal{H}_\varphi)_{\frac{1}{2}, k+\frac{1}{2}} + \left[I_2 + \frac{d\mathcal{D}_2}{dt} \right]_{0, k+\frac{1}{2}} \right\} \\ & + \sum_{k=0}^{N_2-1} (\mathcal{E}_2)_{N_1, k+\frac{1}{2}} \left\{ -(\mathcal{H}_\varphi)_{N_1-\frac{1}{2}, k+\frac{1}{2}} + \left[I_2 + \frac{d\mathcal{D}_2}{dt} \right]_{N_1, k+\frac{1}{2}} \right\} \end{aligned} \quad (23)$$

in which the energy density and $\mathbf{J} \cdot \mathbf{E}$ work are easily recognized on the left-hand side.* On the right-hand side, the $\{\dots\}$ factors are representations of \mathcal{H} at the boundary, so we recognize these sums as the energy flux through the boundaries.

Consider now leap-frog time differencing and spatial continuum.

Define the energy density at time t_n

$$U^n = \frac{\epsilon_0}{2}(\mathbf{E}^n)^2 + \frac{1}{2\mu_0}(\mathbf{B}^{n-\frac{1}{2}} \cdot \mathbf{B}^{n+\frac{1}{2}}) \quad (24)$$

Then a Poynting theorem may be derived:

$$U^{n+1} - U^n = -\Delta t \frac{1}{\mu_0} \nabla \cdot \left[\frac{1}{2}(\mathbf{E}^n + \mathbf{E}^{n+1}) \times \mathbf{B}^{n+\frac{1}{2}} \right] - \Delta t \mathbf{J}^{n+\frac{1}{2}} \cdot \frac{1}{2}(\mathbf{E}^n + \mathbf{E}^{n+1}) \quad (25)$$

As we know must be true, this result does not imply such useful properties as stability, because the magnetic energy as defined here can be negative. For example, when the time step is so large as to produce a Courant-type instability, the fields change sign from time step to step.

However, the existence of this theorem means that errors in the field energy balance, when the magnetic energy is formed using an arithmetic instead of geometric mean, cannot accumulate to values large relative to the magnetic energy; the difference between these magnetic energies density is $-(\mathbf{B}^{n+\frac{1}{2}} - \mathbf{B}^{n-\frac{1}{2}})^2/2\mu_0$.

Now rederive the last boundary flux term in the Poynting theorem (23), with space and time both discrete:

$$\sum_{k=0}^{N_2-1} \frac{1}{2} \left((\mathcal{E}_2)_{N_1, k+\frac{1}{2}}^n + (\mathcal{E}_2)_{N_1, k+\frac{1}{2}}^{n+1} \right) \left\{ -(\mathcal{H}_\varphi)_{N_1-\frac{1}{2}, k+\frac{1}{2}}^{n+\frac{1}{2}} + \left[I_2^{n+\frac{1}{2}} + \frac{\mathcal{D}_2^{n+1} - \mathcal{D}_2^n}{\Delta t} \right]_{N_1, k+\frac{1}{2}} \right\} \quad (26)$$

We make use of this in our discussion of outgoing wave boundary conditions.

Positivity of Field Energy

Here we discuss the conditions under which the field energy is nonnegative,

$$\sum \frac{1}{2} \mathcal{E}_1 \mathcal{D}_1 + \sum \frac{1}{2} \mathcal{E}_2 \mathcal{D}_2 + \sum \frac{1}{2} \mathcal{H}_\varphi \mathcal{B}_\varphi \geq 0$$

This same inequality also arises in the discussion of stability, below.

This imposes conditions on the C^{-1} matrix that are trivial except for the C_\backslash and C_\uparrow terms.

Stability of electromagnetic cavity oscillations

Our discretization provides *provably* neutrally-stable electromagnetic oscillations, that is, neither damping nor instability of vacuum oscillations in a perfectly-conducting cavity.

* It may be interesting to note the relation for the “electrostatic” field energy

$$\frac{1}{2} \sum Q\varphi = \frac{1}{2} \sum \frac{1}{2} \mathcal{E}_1 \mathcal{D}_1 + \frac{1}{2} \sum \frac{1}{2} \mathcal{E}_2 \mathcal{D}_2$$

which follows when the electric field is irrotational by summing (5) times $\varphi_{j,k}$, using (2), and ignoring boundary terms.

For a closed system with diagonal L and C , we find the wave equation

$$\begin{aligned}
-L_{j+\frac{1}{2},k+\frac{1}{2}} \frac{d^2}{dt^2} (\mathcal{H}_\varphi)_{j+\frac{1}{2},k+\frac{1}{2}} &= \frac{1}{C_{j+\frac{1}{2},k}} [(\mathcal{H}_\varphi)_{j+\frac{1}{2},k+\frac{1}{2}} - (\mathcal{H}_\varphi)_{j+\frac{1}{2},k-\frac{1}{2}}] \\
&+ \frac{1}{C_{j+\frac{1}{2},k+1}} [(\mathcal{H}_\varphi)_{j+\frac{1}{2},k+\frac{1}{2}} - (\mathcal{H}_\varphi)_{j+\frac{1}{2},k+\frac{3}{2}}] \\
&+ \frac{1}{C_{j,k+\frac{1}{2}}} [(\mathcal{H}_\varphi)_{j+\frac{1}{2},k+\frac{1}{2}} - (\mathcal{H}_\varphi)_{j-\frac{1}{2},k+\frac{1}{2}}] \\
&+ \frac{1}{C_{j+1,k+\frac{1}{2}}} [(\mathcal{H}_\varphi)_{j+\frac{1}{2},k+\frac{1}{2}} - (\mathcal{H}_\varphi)_{j+\frac{3}{2},k+\frac{1}{2}}]
\end{aligned} \tag{30}$$

To show the stability of vacuum cavity oscillations below the Courant limit, first note that the rhs represents a symmetric operation on (\mathcal{H}_φ) . Then multiply the right-hand-side by $(\mathcal{H}_\varphi)_{j+\frac{1}{2},k+\frac{1}{2}}$ and sum, obtaining

$$\sum \frac{1}{C_{j,k+\frac{1}{2}}} [(\mathcal{H}_\varphi)_{j+\frac{1}{2},k+\frac{1}{2}} - (\mathcal{H}_\varphi)_{j-\frac{1}{2},k+\frac{1}{2}}]^2 + \sum \frac{1}{C_{j+\frac{1}{2},k}} [(\mathcal{H}_\varphi)_{j+\frac{1}{2},k+\frac{1}{2}} - (\mathcal{H}_\varphi)_{j+\frac{1}{2},k-\frac{1}{2}}]^2 \tag{31}$$

which is overtly non-negative. Therefore, when we replace the time derivatives by leap-frog differencing, $\left(\frac{2}{\Delta t} \sin \frac{\omega \Delta t}{2}\right)^2$ is real and is positive for each eigenmode. We have neutral stability for any time step Δt below the threshold for Courant instability as given by the largest eigenvalue.

Most generally, $d^2(\mathcal{H}_\varphi)_{j+\frac{1}{2},k+\frac{1}{2}}/dt^2$ is a linear combination of the $(\mathcal{H}_\varphi)_{j+\frac{1}{2},k+\frac{1}{2}}$. We discuss symmetry and positivity of this linear combination by starting with the time derivative of the Faraday law for $d\mathcal{B}/dt$, multiply by $-(\mathcal{H}'_\varphi)$ and sum, then rearrange the sum, then use Ampere-Maxwell, through these steps:

$$\begin{aligned}
&-\sum_{j,k} (\mathcal{H}'_\varphi)_{j+\frac{1}{2},k+\frac{1}{2}} L_{j+\frac{1}{2},k+\frac{1}{2}} \frac{d^2}{dt^2} (\mathcal{H}_\varphi)_{j+\frac{1}{2},k+\frac{1}{2}} \\
&= -\sum_{j,k} (\mathcal{H}'_\varphi)_{j+\frac{1}{2},k+\frac{1}{2}} \frac{d}{dt} \left((\mathcal{E}_1)_{j+\frac{1}{2},k+1} - (\mathcal{E}_1)_{j+\frac{1}{2},k} - (\mathcal{E}_2)_{j+1,k+\frac{1}{2}} + (\mathcal{E}_2)_{j,k+\frac{1}{2}} \right) \\
&= \sum_{j,k} \left((\mathcal{H}'_\varphi)_{j+\frac{1}{2},k+\frac{1}{2}} - (\mathcal{H}'_\varphi)_{j+\frac{1}{2},k-\frac{1}{2}} \right) \left[\frac{d\mathcal{E}_1}{dt} \right]_{j+\frac{1}{2},k} \\
&\quad - \sum_{j,k} \left((\mathcal{H}'_\varphi)_{j+\frac{1}{2},k+\frac{1}{2}} - (\mathcal{H}'_\varphi)_{j-\frac{1}{2},k+\frac{1}{2}} \right) \left[\frac{d\mathcal{E}_2}{dt} \right]_{j,k+\frac{1}{2}} \\
&= \sum_{j,k} \left[\frac{d\mathcal{D}'_1}{dt} \right]_{j+\frac{1}{2},k} \left[\frac{d\mathcal{E}_1}{dt} \right]_{j+\frac{1}{2},k} + \sum_{j,k} \left[\frac{d\mathcal{D}'_2}{dt} \right]_{j,k+\frac{1}{2}} \left[\frac{d\mathcal{E}_2}{dt} \right]_{j,k+\frac{1}{2}}
\end{aligned} \tag{32}$$

The primed fields \mathcal{H}' , \mathcal{D}' are possibly a different time evolution than the unprimed fields. If the transformation of \mathcal{D} to \mathcal{E} is symmetric, then the last line equals itself with the primes moved to the \mathcal{E} 's. Therefore the first line is equal to itself with the prime moved, and therefore the operator is symmetric. Setting $\mathcal{H}' = \mathcal{H}$, we see that the operator is non-negative if the transformation of \mathcal{D} to \mathcal{E} is non-negative. Given symmetry and non-negativity of the capacitance transform in Eq. (15), we again find neutral stability of the vacuum oscillations, for time steps below the Courant limit.

Madsen [6] describes how instability could take very long simulation times to appear, $\sim 20,000$ steps, enough time for signals to transit the computational domain many times, in an earlier EM scheme he calls MFV. He also reports that the DSI method [6] has not shown this slow instability, and that very long simulation times are needed to verify stability. However, Brandon and Rambo have since found slow instability in DSI [7]. In contrast, the scheme presented here provides analytic assurance of stability for time

steps smaller than the Courant limit, and promises to provide a quicker check on stability, amounting to determination of the Courant limit, as follows:

The Courant limit can be accurately estimated by an iteration that is relatively cheap, performed during problem setup: Cycle the EM fields using a time step Δt_L that is many times larger than the light transit time across the smallest cell, starting with random noise in the field arrays, and setting currents = 0. The fields will begin to grow rapidly, perhaps in a region of small or distorted cells. Monitor the ratio R of the largest \mathcal{E} to the value at the preceding cycle. As the fields grow (but before numerical overflow occurs!), R provides an increasingly accurate measure of the highest frequency that the mesh can generate, ω_L , given by $(\omega_L \Delta t_L)^2 = R$. The Courant limit for the time step is then $2/\omega_L$.

Keep in mind that boundary conditions can undermine these nice features.

Evaluation of the L 's and C 's

Nearly-orthogonal cells in r, z geometry

Here are initial suggestions for this important special case:

In the capacitance the distance is denoted $(h_1 \Delta x_1)_{j+\frac{1}{2},k}$ and is evaluated as exactly the length between mesh points (j, k) and $(j+1, k)$

$$(h_1 \Delta x_1)_{j+\frac{1}{2},k} = [(r_{j+1,k} - r_{j,k})^2 + (z_{j+1,k} - z_{j,k})^2]^{1/2}, \quad j = 0, N_z - 1, \quad k = 0, N_r. \quad (40)$$

The area, denoted $(rh_1 \Delta x_1)_{j,k+\frac{1}{2}}$, is exactly the area of a section of cone connecting points in the middle between the mesh points:

$$(rh_1 \Delta x_1)_{j,k+\frac{1}{2}} = (2\pi)^{\frac{1}{2}} (r_{j+\frac{1}{2},k+\frac{1}{2}} + r_{j-\frac{1}{2},k+\frac{1}{2}}) \left[(r_{j+\frac{1}{2},k+\frac{1}{2}} - r_{j-\frac{1}{2},k+\frac{1}{2}})^2 + (z_{j+\frac{1}{2},k+\frac{1}{2}} - z_{j-\frac{1}{2},k+\frac{1}{2}})^2 \right]^{1/2} \quad (41)$$

for $j = 1, N_z - 1, k = 0, N_r - 1$, where

$$4r_{j+\frac{1}{2},k+\frac{1}{2}} = r_{j,k} + r_{j+1,k} + r_{j,k+1} + r_{j+1,k+1} \quad (42)$$

(the definition chosen is somewhat arbitrary but plausible), and

$$(rh_1 \Delta x_1)_{0,k+\frac{1}{2}} = (2\pi)^{\frac{1}{2}} (r_{0,k+\frac{1}{2}} + r_{\frac{1}{2},k+\frac{1}{2}}) \left[(r_{\frac{1}{2},k+\frac{1}{2}} - r_{0,k+\frac{1}{2}})^2 + (z_{\frac{1}{2},k+\frac{1}{2}} - z_{0,k+\frac{1}{2}})^2 \right]^{1/2} \quad (43)$$

where $2r_{0,k+\frac{1}{2}} = r_{0,k} + r_{0,k+1}$, etc. Then the capacitances are, for example

$$C_{j+\frac{1}{2},k} = \epsilon_0 \frac{(rh_2 \Delta x_2)_{j+\frac{1}{2},k}}{(h_1 \Delta x_1)_{j+\frac{1}{2},k}}. \quad (44)$$

For the inductance, the length is the circumference corresponding to radius $r_{j+\frac{1}{2},k+\frac{1}{2}}$. The cell area, denoted $(h_1 \Delta x_1 h_2 \Delta x_2)_{j+\frac{1}{2},k+\frac{1}{2}}$, is exactly the area of the quadrilateral cell, which can be written

$$(h_1 \Delta x_1 h_2 \Delta x_2)_{j+\frac{1}{2},k+\frac{1}{2}} = \frac{1}{2} [(z_{j+1,k+1} - z_{j,k})(r_{j,k+1} - r_{j+1,k}) - (r_{j+1,k+1} - r_{j,k})(z_{j,k+1} - z_{j+1,k})] \quad (45)$$

Then the inductance is

$$L_{j+\frac{1}{2},k+\frac{1}{2}} = \mu_0 \frac{(h_1 \Delta x_1 h_2 \Delta x_2)_{j+\frac{1}{2},k+\frac{1}{2}}}{r_{j+\frac{1}{2},k+\frac{1}{2}}}. \quad (46)$$

(In cylindrical coordinates with uniform spacing, the preceding reduces to what's in [8]).

Non-orthogonal cells in x, y geometry

For now consider a regular mesh of parallelogram cells whose mesh node j, k is located at position

$$\mathbf{X}_{j,k} = j\mathbf{X}_1 + k\mathbf{X}_2 \quad (50)$$

and edge centers located at $\mathbf{X}_{j+\frac{1}{2},k} = (j+\frac{1}{2})\mathbf{X}_1 + k\mathbf{X}_2$, etc. The results here are also a guide for an irregular mesh whose cell shapes and orientations vary smoothly.

We can find the capacitances and inductances by considering a magnetic field that varies linearly with position:

$$\mathcal{H}_{z,j+\frac{1}{2},k+\frac{1}{2}} = \mathbf{h} \cdot \mathbf{X}_{j+\frac{1}{2},k+\frac{1}{2}} \quad (51)$$

The magnetic flux through a cell is given by \mathcal{H}_z at the center times the cell area $A = \hat{\mathbf{z}} \cdot \mathbf{X}_1 \times \mathbf{X}_2$, therefore

$$L_{j+\frac{1}{2},k+\frac{1}{2}} = \mu_0 A \quad (52)$$

To find the capacitances, consider the time derivative of the electric field:

$$\epsilon_0 \frac{\partial \mathbf{E}}{\partial t} = \nabla \times \mathbf{H} = \nabla \mathcal{H}_z \times \hat{\mathbf{z}} = \mathbf{h} \times \hat{\mathbf{z}}$$

from which

$$\epsilon_0 \dot{\mathcal{E}}_1 = \mathbf{X}_1 \cdot \dot{\mathbf{E}} = \mathbf{h} \cdot \hat{\mathbf{z}} \times \mathbf{X}_1, \quad \epsilon_0 \dot{\mathcal{E}}_2 = \mathbf{h} \cdot \hat{\mathbf{z}} \times \mathbf{X}_2 \quad (53ab)$$

Assume $\mathbf{X}_1 \cdot \mathbf{X}_2 \geq 0$ and that the only nonzero off-diagonal capacitances are those between nearest cell sides

$$C_{\setminus} \equiv C_{j+\frac{1}{2},k,j,k+\frac{1}{2}} \equiv C_{j,k+\frac{1}{2},j+\frac{1}{2},k} \quad (54)$$

where the second equality arises naturally in the following derivation.

Using (4) and (15),

$$\begin{aligned} \dot{\mathcal{E}}_{1,j+\frac{1}{2},k} &= C_-^{-1} \dot{\mathcal{D}}_{1,j+\frac{1}{2},k} + C_{\setminus}^{-1} (\dot{\mathcal{D}}_{2,j,k+\frac{1}{2}} + \dot{\mathcal{D}}_{2,j+1,k-\frac{1}{2}}) \\ &= C_-^{-1} (\mathcal{H}_{z,j+\frac{1}{2},k+\frac{1}{2}} - \mathcal{H}_{z,j+\frac{1}{2},k-\frac{1}{2}}) \\ &\quad - C_{\setminus}^{-1} (\mathcal{H}_{z,j+\frac{1}{2},k+\frac{1}{2}} - \mathcal{H}_{z,j-\frac{1}{2},k+\frac{1}{2}} + \mathcal{H}_{z,j+\frac{3}{2},k-\frac{1}{2}} - \mathcal{H}_{z,j+\frac{1}{2},k-\frac{1}{2}}) \end{aligned} \quad (55a)$$

$$\begin{aligned} \dot{\mathcal{E}}_{2,j,k+\frac{1}{2}} &= C_{\setminus}^{-1} \dot{\mathcal{D}}_{2,j,k+\frac{1}{2}} + C_{\setminus}^{-1} (\dot{\mathcal{D}}_{1,j+\frac{1}{2},k} + \dot{\mathcal{D}}_{1,j-\frac{1}{2},k+1}) \\ &= -C_{\setminus}^{-1} (\mathcal{H}_{z,j+\frac{1}{2},k+\frac{1}{2}} - \mathcal{H}_{z,j-\frac{1}{2},k+\frac{1}{2}}) \\ &\quad + C_{\setminus}^{-1} (\mathcal{H}_{z,j+\frac{1}{2},k+\frac{1}{2}} - \mathcal{H}_{z,j+\frac{1}{2},k-\frac{1}{2}} + \mathcal{H}_{z,j-\frac{1}{2},k+\frac{3}{2}} - \mathcal{H}_{z,j-\frac{1}{2},k+\frac{1}{2}}) \end{aligned} \quad (55b)$$

where $C_- = C_{j+\frac{1}{2},k}$, $C_{\setminus} = C_{j,k+\frac{1}{2}}$

$$\dot{\mathcal{E}}_1 = C_-^{-1} \mathbf{h} \cdot \mathbf{X}_2 - C_{\setminus}^{-1} 2\mathbf{h} \cdot \mathbf{X}_1, \quad \dot{\mathcal{E}}_2 = -C_{\setminus}^{-1} \mathbf{h} \cdot \mathbf{X}_1 + C_{\setminus}^{-1} 2\mathbf{h} \cdot \mathbf{X}_2$$

for all \mathbf{h} , therefore, on comparing to (53) we have

$$\hat{\mathbf{z}} \times \mathbf{X}_1 = \frac{\epsilon_0}{C_-} \mathbf{X}_2 - \frac{\epsilon_0}{C_{\setminus}} 2\mathbf{X}_1, \quad \hat{\mathbf{z}} \times \mathbf{X}_2 = -\frac{\epsilon_0}{C_{\setminus}} \mathbf{X}_1 + \frac{\epsilon_0}{C_{\setminus}} 2\mathbf{X}_2$$

By applying the operations $\mathbf{X}_1 \cdot$ and $\hat{\mathbf{z}} \cdot \mathbf{X}_1 \times$ to the first equation, and $\mathbf{X}_2 \cdot$ and $\hat{\mathbf{z}} \cdot \mathbf{X}_2 \times$ to the second equation, we then find

$$C_- = \epsilon_0 \frac{A}{X_1^2}, \quad C_{\setminus} = \epsilon_0 \frac{A}{X_2^2}, \quad C_{\setminus} = 2\epsilon_0 \frac{A}{\mathbf{X}_1 \cdot \mathbf{X}_2} \quad (56abc)$$

Note that the coupling of \mathcal{D} to \mathcal{E} in (55) reduces to the form of (11) when $\mathbf{X}_2 \perp \mathbf{X}_1$, as expected. (It is C_{\setminus}^{-1} that vanishes, not C_{\setminus} !) Note that the cross-coupling C_{\setminus}^{-1} is negative if $\mathbf{X}_1 \cdot \mathbf{X}_2 < 0$, i.e. if the angle between \mathbf{X}_1 and \mathbf{X}_2 is obtuse rather than acute (so that we should have worked with C_{\setminus}^{-1} instead).

We return to this subject in the discussion of the dispersion relation.

Materials

In an isotropic dielectric, replace the vacuum ϵ_0 by the dielectric's ϵ . Some dispersive dielectrics can be modeled by adding time derivative terms.

In an isotropic resistive medium, you could create a current $I_1^{n+\frac{1}{2}}$ suitably proportional to $\frac{1}{2}(\mathcal{E}_1^n + \mathcal{E}_1^{n+1})$; likewise $I_2^{n+\frac{1}{2}}$. If you are using Q , e.g. for a divergence correction, then you will need to update Q using Eq. (5) including the resistive current. If the resistance is anisotropic, e.g. if one is faking a helically-conducting layer, then I_1 will need to be driven by a linear combination of \mathcal{E}_1 and some spatial average of neighboring \mathcal{E}_2 values, since I_1 is known at different positions than is \mathcal{E}_2 . This linear combination could be combined with the C transformation, so that the resistive I is given in terms of \mathcal{D} . Inserted into Eqs. (4,6) with leap-frog time differencing, one now has linear equations to solve for the time-advanced \mathcal{D} . The linear equations can be avoided if the time step is small enough by expressing $I^{n+\frac{1}{2}}$ in terms of \mathcal{D}^n rather than the time-centered $\frac{1}{2}(\mathcal{D}^n + \mathcal{D}^{n+1})$. Is all this perfectly transparent?

In a nonlinear magnetic material with hysteresis, you will have to provide an algorithm to find \mathcal{H} from the history of \mathcal{B} .

Dispersion Relations

Let's derive a dispersion relation for sinusoidal waves on an infinite mesh of parallelograms, Eq. (50). Let

$$\mathcal{H}_{z,j+\frac{1}{2},k+\frac{1}{2}} = \mathcal{H} \exp(ik \cdot \mathbf{X}_{j+\frac{1}{2},k+\frac{1}{2}}), \quad \mathcal{E}_{1,j+\frac{1}{2},k} = \mathcal{E}_1 \exp(ik \cdot \mathbf{X}_{j+\frac{1}{2},k}), \quad \mathcal{E}_{2,j,k+\frac{1}{2}} = \mathcal{E}_2 \exp(ik \cdot \mathbf{X}_{j,k+\frac{1}{2}}) \quad (57)$$

in place of Eq. (51). From (3) and (55),

$$\begin{aligned} L\ddot{\mathcal{H}} &= \dot{\mathcal{E}}_1 2i \sin \frac{1}{2}k \cdot \mathbf{X}_2 - \dot{\mathcal{E}}_2 2i \sin \frac{1}{2}k \cdot \mathbf{X}_1 \\ \dot{\mathcal{E}}_1/\mathcal{H} &= C_1^{-1} 2i \sin k \cdot \mathbf{X}_2 - C_1^{-1} 2i (\sin \frac{1}{2}k \cdot \mathbf{X}_1) 2 \cos \frac{1}{2}k \cdot (\mathbf{X}_2 - \mathbf{X}_1) \\ \dot{\mathcal{E}}_2/\mathcal{H} &= -C_1^{-1} 2i \sin \frac{1}{2}k \cdot \mathbf{X}_1 + C_1^{-1} 2i (\sin \frac{1}{2}k \cdot \mathbf{X}_2) 2 \cos \frac{1}{2}k \cdot (\mathbf{X}_2 - \mathbf{X}_1) \end{aligned} \quad (58abc)$$

The dispersion relation is then

$$-L\ddot{\mathcal{H}}/\mathcal{H} = C_1^{-1} 4 \sin^2 \frac{1}{2}k \cdot \mathbf{X}_1 + C_1^{-1} 4 \sin^2 \frac{1}{2}k \cdot \mathbf{X}_2 - C_1^{-1} 8 (\sin \frac{1}{2}k \cdot \mathbf{X}_1 \sin \frac{1}{2}k \cdot \mathbf{X}_2) 2 \cos \frac{1}{2}k \cdot (\mathbf{X}_2 - \mathbf{X}_1) \quad (59)$$

For small k ,

$$-L\ddot{\mathcal{H}}/\mathcal{H} = C_1^{-1} (k \cdot \mathbf{X}_1)^2 + C_1^{-1} (k \cdot \mathbf{X}_2)^2 - 4C_1^{-1} (k \cdot \mathbf{X}_1)(k \cdot \mathbf{X}_2)$$

Compare with the identity

$$A^2 k^2 = X_2^2 (k \cdot \mathbf{X}_1)^2 + X_1^2 (k \cdot \mathbf{X}_2)^2 - 2(\mathbf{X}_1 \cdot \mathbf{X}_2)(k \cdot \mathbf{X}_1)(k \cdot \mathbf{X}_2)$$

and (52), where $A = \hat{z} \cdot \mathbf{X}_1 \times \mathbf{X}_2$ is the cell area. We find that we approach the correct result, $-\ddot{\mathcal{H}}/\mathcal{H} = k^2/\mu_0\epsilon_0$ for small k if we use (56) for the capacitances. The dispersion relation therefore provides an alternate derivation of (56).

The dispersion relation now is

$$-\epsilon_0\mu_0 A^2 \ddot{\mathcal{H}} = 4\mathcal{H} [X_2^2 \sin^2 \frac{1}{2}k \cdot \mathbf{X}_1 + X_1^2 \sin^2 \frac{1}{2}k \cdot \mathbf{X}_2 - 2\mathbf{X}_1 \cdot \mathbf{X}_2 (\sin \frac{1}{2}k \cdot \mathbf{X}_1 \sin \frac{1}{2}k \cdot \mathbf{X}_2) \cos \frac{1}{2}k \cdot (\mathbf{X}_2 - \mathbf{X}_1)] \quad (591)$$

Contours of $-\epsilon_0\mu_0 \ddot{\mathcal{H}}/\mathcal{H}$ are shown in Figure 1 for a case in which $\mathbf{X}_1 = (1, 0)$, $\mathbf{X}_2 = (.5, .9)$. The spacing of the contour levels is quadratic, so that the desired result is concentric circles of linearly-increasing radius, corresponding to contours of k^2 .

In contrast, Figure 2 shows the dispersion when the cross term with coefficient C_1^{-1} is omitted, for which the dispersion relation becomes $-\epsilon_0\mu_0 A^2 \ddot{\mathcal{H}} = 4\mathcal{H} [X_2^2 \sin^2 \frac{1}{2}k \cdot \mathbf{X}_1 + X_1^2 \sin^2 \frac{1}{2}k \cdot \mathbf{X}_2]$ Note that the contours are ellipses rather than circles, even for small k . This anisotropy is a *zero-order* error – it remains even when the mesh is made indefinitely fine.

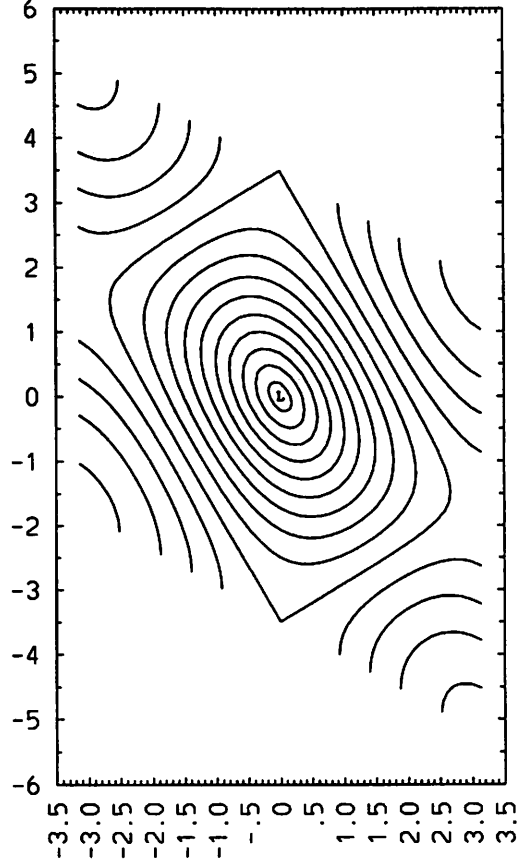


Figure 2. Contours of $-\epsilon_0\mu_0\tilde{\mathcal{H}}/\mathcal{H}$ as given by Eq. (59) with no cross terms C_i or C_j .

Note that the dispersion is anisotropic even at long wavelengths. Only the principal Brillouin zone is shown; the contours are periodic in \mathbf{k} .

In the code we use a time average for \mathcal{E} and the Ampere-Maxwell equation to get \mathcal{H} at the boundary:

$$\frac{1}{2} \left((\mathcal{E}_2)_{N_1, k+\frac{1}{2}}^n + (\mathcal{E}_2)_{N_1, k+\frac{1}{2}}^{n+1} \right) = \mu_0 c \frac{(h_2 \Delta x_2)_{N_1, k+\frac{1}{2}}}{2\pi r_{N_1-\frac{1}{2}, k+\frac{1}{2}}} \left\{ (\mathcal{H}_\varphi)_{N_1-\frac{1}{2}, k+\frac{1}{2}}^{n+\frac{1}{2}} - \left[I_2^{n+\frac{1}{2}} + \frac{\mathcal{D}_2^{n+1} - \mathcal{D}_2^n}{\Delta t} \right]_{N_1, k+\frac{1}{2}} \right\} \quad (61)$$

Comparing to the Poynting theorem, we see that the boundary term in (26) is the negative of a quantity squared, so this boundary condition guarantees that energy can flow only out! Perhaps this helps account for its untempermental behavior as compared to more accurate boundary conditions such as Lindman's that however sometimes fail.

Mesh Coordinates

There is a mapping of *mesh coordinates* x_1, x_2 to z, r . The mapping is continuous, and linear in each of x_1, x_2 (bilinear). Cell boundaries are quadrilaterals on whose sides the mapping functions x_1 and x_2 both take on integer values; the 3D cell is formed by sweeping the quadrilateral a unit distance in z or rotating in about the z axis. Here, the mapping has constant gradient inside each cell.

Let \mathbf{x} or \mathbf{X} be either the vector (z, r) or the vector (x, y) . The mesh points are at $\mathbf{X}_{j,k}$.

The weights (w_1, w_2) are the fractional parts of the particle mesh coordinate x_1, x_2 and lie in the interval $[0, 1)$. Their meaning here is that the position in a cell is given by

$$\mathbf{x} = (1 - w_1)(1 - w_2)\mathbf{X}_{j,k} + (1 - w_1)w_2\mathbf{X}_{j,k+1} + w_1(1 - w_2)\mathbf{X}_{j+1,k} + w_1w_2\mathbf{X}_{j+1,k+1} \quad (70)$$

Solution for (w_1, w_2) given \mathbf{x} is discussed by Seldner and Westermann [9,10]. The indices j, k are the largest integers $\leq x_1, x_2$.

Electric field interpolation

We need to find an electric field at the positions of the particles. Here we show the field as found from a variational principle, then discuss a bilinear representation.

For the case of rectangular cells, see [8] chapter 10, [11] section 5-5, and [12]. We want to get expressions for the field in terms of the quantities used in these notes, such as \mathcal{E} . It suffices to consider an irrotational electric field. Take the potential to be bilinear in (w_1, w_2) in each cell.

$$\frac{\partial \mathbf{x}}{\partial w_1} \cdot \frac{\partial \varphi}{\partial \mathbf{x}} = \frac{\partial \varphi}{\partial w_1}, \quad \frac{\partial \mathbf{x}}{\partial w_2} \cdot \frac{\partial \varphi}{\partial \mathbf{x}} = \frac{\partial \varphi}{\partial w_2} \quad (80)$$

with

$$\frac{\partial \mathbf{x}}{\partial w_1} = (1 - w_2)(\mathbf{X}_{j+1,k} - \mathbf{X}_{j,k}) + w_2(\mathbf{X}_{j+1,k+1} - \mathbf{X}_{j,k+1}) \quad (81a)$$

$$\frac{\partial \mathbf{x}}{\partial w_2} = (1 - w_1)(\mathbf{X}_{j,k+1} - \mathbf{X}_{j,k}) + w_1(\mathbf{X}_{j+1,k+1} - \mathbf{X}_{j+1,k}) \quad (81b)$$

In terms of its corner values,

$$\begin{aligned} \frac{\partial \varphi}{\partial w_1} &= (1 - w_2)(\varphi_{j+1,k} - \varphi_{j,k}) + w_2(\varphi_{j+1,k+1} - \varphi_{j,k+1}) \\ &= -(1 - w_2)\mathcal{E}_{1,j+\frac{1}{2},k} - w_2\mathcal{E}_{1,j+\frac{1}{2},k+1} \end{aligned} \quad (82a)$$

$$\begin{aligned} \frac{\partial \varphi}{\partial w_2} &= (1 - w_1)(\varphi_{j,k+1} - \varphi_{j,k}) + w_1(\varphi_{j+1,k+1} - \varphi_{j+1,k}) \\ &= -(1 - w_1)\mathcal{E}_{2,j,k+\frac{1}{2}} - w_1\mathcal{E}_{2,j+1,k+\frac{1}{2}} \end{aligned} \quad (82b)$$

So we have the values of $-\mathbf{E} = \nabla \varphi \equiv \partial \varphi / \partial \mathbf{x}$ dotted with 2 vectors. The solution is

$$\begin{aligned} A\mathbf{E} &= -\left(\hat{\mathbf{z}} \times \frac{\partial \mathbf{x}}{\partial w_1}\right) \frac{\partial \varphi}{\partial w_2} + \left(\hat{\mathbf{z}} \times \frac{\partial \mathbf{x}}{\partial w_2}\right) \frac{\partial \varphi}{\partial w_1} \\ &= \left(\hat{\mathbf{z}} \times \frac{\partial \mathbf{x}}{\partial w_1}\right) \left[(1 - w_1)\mathcal{E}_{2,j,k+\frac{1}{2}} + w_1\mathcal{E}_{2,j+1,k+\frac{1}{2}}\right] - \left(\hat{\mathbf{z}} \times \frac{\partial \mathbf{x}}{\partial w_2}\right) \left[(1 - w_2)\mathcal{E}_{1,j+\frac{1}{2},k} + w_2\mathcal{E}_{1,j+\frac{1}{2},k+1}\right] \end{aligned} \quad (83b)$$

where

$$A = \hat{\mathbf{z}} \cdot \left(\frac{\partial \mathbf{x}}{\partial w_1} \times \frac{\partial \mathbf{x}}{\partial w_2} \right) \quad (84)$$

In this second form, the result holds whether or not the field is irrotational.

Current and charge collection

The contribution of charge q_i to grid charge Q can be chosen to be bilinear in its mesh coordinates x_1, x_2 :

$$\begin{aligned} Q_{j,k} &= q_i(1-w_1)(1-w_2) \\ Q_{j+1,k} &= q_i w_1(1-w_2) \\ Q_{j,k+1} &= q_i(1-w_1)w_2 \\ Q_{j+1,k+1} &= q_i w_1 w_2 \end{aligned} \quad (100)$$

where w_1 is the fractional part of x_1 , and j is the integral part of x_1 .

Current I_1, I_2 due to a particle is found from the *change* in its mesh coordinate x_1, x_2 . This is explicitly the case when a charge-conserving current collection is used. Consider the change $\Delta Q = Q^{n+1} - Q^n$ due to a change in x_1, x_2 when the particle remains in the same cell:

$$\begin{aligned} \Delta Q_{j,k} &= q_i(-\Delta w_1(1-\bar{w}_2) - (1-\bar{w}_1)\Delta w_2) \\ \Delta Q_{j+1,k} &= q_i(\Delta w_1(1-\bar{w}_2) - \bar{w}_1\Delta w_2) \\ \Delta Q_{j,k+1} &= q_i(-\Delta w_1\bar{w}_2 + (1-\bar{w}_1)\Delta w_2) \\ \Delta Q_{j+1,k+1} &= q_i(\Delta w_1\bar{w}_2 + \bar{w}_1\Delta w_2) \end{aligned} \quad (101)$$

where $\bar{w}_1 = \frac{1}{2}(w_1^{n+1} + w_1^n)$ and $\Delta w_1 = (w_1^{n+1} - w_1^n)$, et cetera.

Currents consistent with these changes of Q and the continuity equation are

$$\begin{aligned} \Delta t I_{1,j+\frac{1}{2},k} &= q_i \Delta w_1 (1 - \bar{w}_2) \\ \Delta t I_{1,j+\frac{1}{2},k+1} &= q_i \Delta w_1 \bar{w}_2 \\ \Delta t I_{2,j,k+\frac{1}{2}} &= q_i \Delta w_2 (1 - \bar{w}_1) \\ \Delta t I_{2,j+1,k+\frac{1}{2}} &= q_i \Delta w_2 \bar{w}_1 \end{aligned} \quad (102)$$

Note these are not unique, but I suspect they are the simplest possibility. These are the same as one obtains from Morse and Nielson [13,14] in a rectangular mesh, and are the same as come out of Galerkin derivations.

Enforcing Gauss' Law

If a non-conservative current collection is used, the updated \mathcal{D} 's will not exactly correspond to Q in Gauss' law (5). Here is how a Boris correction [8, chapter 15] could be done when there are only diagonal capacitance couplings:

We update \mathcal{D} using the leap-frog version of (4); the new \mathcal{D} 's do not satisfy (5). \mathcal{D} and \mathcal{E} are related by (11). We apply an irrotational correction to \mathcal{E} of the form

$$\mathcal{E}'_{1j+\frac{1}{2},k} = \mathcal{E}_{1j+\frac{1}{2},k} - \psi_{j+1,k} + \psi_{j,k}, \quad \mathcal{E}'_{2j,k+\frac{1}{2}} = \mathcal{E}_{2j,k+\frac{1}{2}} - \psi_{j,k+1} + \psi_{j,k} \quad (111)$$

To find ψ we say that the \mathcal{D} 's corresponding to the adjusted \mathcal{E}' do satisfy (5). Using (111) and (11) in (5), we derive the equation

$$\begin{aligned} C_{j+\frac{1}{2},k}(\psi_{j,k} - \psi_{j+1,k}) + C_{j-\frac{1}{2},k}(\psi_{j,k} - \psi_{j-1,k}) + C_{j,k+\frac{1}{2}}(\psi_{j,k} - \psi_{j,k+1}) + C_{j,k-\frac{1}{2}}(\psi_{j,k} - \psi_{j,k-1}) \\ = C_{j+\frac{1}{2},k}\mathcal{E}_{1,j+\frac{1}{2},k} - C_{j-\frac{1}{2},k}\mathcal{E}_{1,j-\frac{1}{2},k} + C_{j,k+\frac{1}{2}}\mathcal{E}_{2,j,k+\frac{1}{2}} - C_{j,k-\frac{1}{2}}\mathcal{E}_{2,j,k-\frac{1}{2}} - Q_{j,k} \end{aligned} \quad (112)$$

This corresponds to (16) in [15], but using the variables we advocate in this document. (112) is a Poisson equation with a symmetric, positive definite operator for which many solution methods appear in the literature.

Approximate methods to satisfy (5) are compared in [15], but not for the non-diagonal capacitance used here for non-orthogonal mesh. We have a simple transformation (15) of \mathcal{D} to \mathcal{E} in terms of inverse

capacitances. Depending on the sparsity pattern for $(C^{-1})^{-1}$, the inverse transformation of \mathcal{E} to \mathcal{D} may not be at all simple. In that case, solution of a Poisson's equation for a correction potential is made more difficult.

The use of a correction potential was to ensure that the solenoidal part of \mathbf{E} , that participates in electromagnetic waves, would not be changed. If this is not sacred, we can consider correcting \mathcal{D} , which is very simple.

Acknowledgements

This research was supported by the Air Force Office of Scientific Research under grant F49620-92-J0487. Discussions with C. K. Birdsall, S. Brandon, K. Cartwright, N. T. Gladd, P. Mardahl, W. Peter, P. Rambo, and V. Vahedi are gratefully acknowledged. The author especially thanks J. P. Verboncoeur, the principal author of the OOPIC code physics, for which this work was done.

References

1. A. B. Langdon, "On Enforcing Conservation Laws in Electromagnetic Particle-In-Cell Codes", in the proceedings of the 14th International Conference on the Numerical Simulation of Plasmas, Annapolis, Maryland, 3-6 September 1991.
2. J. Eastwood, AFOSR workshop, George Mason University, Oct. 1992.
3. J. P. Verboncoeur, A. B. Langdon, and H. T. Gladd, "An Object-Oriented Electromagnetic PIC code", *Comp. Phys. Comm.* **87**, 199-211 (1995).
4. J. Eastwood, R. W. Hockney, and W. Arter, "General Geometry PIC for MIMD Computers", *Comput. Phys. Commun.* **87**, 155-178 (1995).
5. P. Rambo, in the proceedings of the 14th International Conference on the Numerical Simulation of Plasmas, Annapolis, Maryland, 3-6 September 1991.
6. N. I. Madsen, "Divergence Preserving Discrete Surface Integral Methods for Maxwell's Curl Equations Using Non-Orthogonal Unstructured Grids", LLNL preprint UCRL-JC-109787, February 1992, submitted to *J. Comput. Phys.*
7. S. T. Brandon and P. W. Rambo, "Stability of the DSI Electromagnetic Update Algorithm on a Chevron Grid," 22nd IEEE Int. Conf. on Plasma Sci., June 5-8, 1995.
8. C. K. Birdsall and A. B. Langdon, *Plasma Physics Via Computer Simulation*, McGraw-Hill, New York, 1985. reprinted by Adam-Hilger/IOP Publishing, 1991.
9. D. Seldner and T. Westermann, "Algorithms for Interpolation and Localization in Irregular 2D Meshes", *J. Comput. Phys.* **79**, 1 (1988).
10. T. Westermann, "Localization Schemes in 2D Boundary-Fitted Grids", *J. Comput. Phys.* **101**, 307 (1992).
11. R. W. Hockney and J. W. Eastwood, *Computer Simulation Using Particles*, McGraw-Hill, New York, 1981, reprinted by Adam-Hilger/IOP Publishing, 1988.
12. H. R. Lewis, "Application of Hamilton's Principle to the Numerical Analysis of Vlasov Plasmas", in *Methods in Computational Physics*, ed. by B. Alder, S. Fernbach and M. Rote nberg (Academic Press, New York), Vol. 9, 1970.
13. R. L. Morse and C. W. Nielson, "Numerical Simulation of the Weibel Instability in One and Two Dimensions", *Phys. Fluids* **14** 830-840 (1971).

14. J. Villasenor and O. Buneman, "Rigorous Charge Conservation for Local Electromagnetic Field Solvers", *Comput. Phys. Commun.* **69**, 306-316 (1992).
15. A. B. Langdon, "On Enforcing Gauss' Law in Electromagnetic Particle-in-Cell Codes", *Comput. Phys. Commun.* **70**, 447-450 (1992).